

Supplementary Information for: Topological properties of Floquet winding bands in a photonic lattice

I. CALCULATION OF THE BAND STRUCTURE

By applying the Floquet-Bloch ansatz to Eq. (1) in the main text and solving the determinant problem we obtain the solution for the energies of the bands E_{\pm} :

$$E_{\pm}(k, \varphi) = \pm \arccos[\cos \theta_1 \cos \theta_2 \cos(k + K\varphi) - \sin \theta_1 \sin \theta_2 \cos(\Delta\varphi)] + K\varphi,$$

where $\varphi_{1,2} = c_{1,2}\varphi$, $K \equiv (c_1 + c_2)/2$, $\Delta \equiv (c_1 - c_2)/2$. In this work we consider the case of integer K and Δ , which makes the period along the φ direction equal to 2π . The last term $K\varphi$ emphasizes the fact that each band winds K times along the quasienergy axis when φ is changed by 2π .

II. DERIVATION OF THE FLOQUET EVOLUTION OPERATOR

For the Floquet period of 2 steps the evolution of the system in real space can be written as

$$\Psi(m+2) = U\Psi(m), \quad (\text{S1})$$

where

$$\Psi(m) = \begin{pmatrix} \dots \\ \alpha_n^m \\ \beta_n^m \\ \alpha_{n+2}^m \\ \beta_{n+2}^m \\ \dots \end{pmatrix} \quad (\text{S2})$$

is a vector representing the state of the system in real space at time step m , and

$$U = \sum_{x_i, y_j} U_{x_i \rightarrow y_j} |y_j\rangle \langle x_i| \quad (\text{S3})$$

is the real-space Floquet evolution operator. Here $|x_i\rangle$ and $|y_j\rangle$, where $x, y \in \{\alpha, \beta\}$ and i, j are the site number, represent a vector Ψ with $x_i = 1$ (or $y_j = 1$) and all the other components equal to zero. Non-zero matrix elements of U can be found from the evolution equation (Eq. (1) of the main text):

$$\begin{aligned} U_{\alpha_n \rightarrow \beta_n} &= is_1 R e^{i\Delta\varphi} & U_{\beta_n \rightarrow \alpha_n} &= is_1 R e^{-i\Delta\varphi} \\ U_{\beta_n \rightarrow \alpha_{n+2}} &= is_2 R e^{iK\varphi} & U_{\alpha_n \rightarrow \beta_{n-2}} &= is_2 R e^{-iK\varphi} \\ U_{\alpha_n \rightarrow \alpha_{n+2}} &= s_3 R e^{iK\varphi} & U_{\beta_n \rightarrow \beta_{n-2}} &= s_3 R e^{-iK\varphi} \\ U_{\beta_n \rightarrow \beta_n} &= -s_4 R e^{i\Delta\varphi} & U_{\alpha_n \rightarrow \alpha_n} &= -s_4 R e^{-i\Delta\varphi} \end{aligned}$$

where $s_1 = \cos \theta_1 \sin \theta_2$, $s_2 = \sin \theta_1 \cos \theta_2$, $s_3 = \cos \theta_1 \cos \theta_2$, $s_4 = \sin \theta_1 \sin \theta_2$, and $R = e^{iK\varphi}$.

To obtain the Floquet evolution operator in reciprocal space, we can use the Floquet-Bloch ansatz and substitute it into the evolution equation. This gives

$$U_F(k, \varphi) = \begin{pmatrix} e^{i(\varphi_1 + \varphi_2)} e^{-ik} \cos \theta_1 \cos \theta_2 & - e^{i\varphi_2} \sin \theta_1 \sin \theta_2 & i e^{i(\varphi_1 + \varphi_2)} e^{-ik} \sin \theta_1 \cos \theta_2 & + i e^{i\varphi_2} \cos \theta_1 \sin \theta_2 \\ i e^{ik} \sin \theta_1 \cos \theta_2 & + i e^{i\varphi_1} \cos \theta_1 \sin \theta_2 & e^{ik} \cos \theta_1 \cos \theta_2 & - e^{i\varphi_1} \sin \theta_1 \sin \theta_2 \end{pmatrix}. \quad (\text{S4})$$

It can be seen that the Floquet evolution operator can be factorized in a sequential manner

$$U_F(k, \varphi) = D_2 B_2(k) S_2 D_1 B_1(k) S_1 \quad (\text{S5})$$

where $S_{1,2} = S(\theta_{1,2})$ are scattering matrices representing the action of the beamsplitter,

$$S(\theta) = \begin{pmatrix} \cos \theta & i \sin \theta \\ i \sin \theta & \cos \theta \end{pmatrix}, \quad (\text{S6})$$

$B_{1,2}(k)$ are translation operators

$$B_1(k) = \begin{pmatrix} 1 & 0 \\ 0 & e^{ik} \end{pmatrix}, B_2(k) = \begin{pmatrix} e^{-ik} & 0 \\ 0 & 1 \end{pmatrix}, \quad (\text{S7})$$

and $D_{1,2}$ correspond to the phase shift on odd and even steps:

$$D_{1,2} = \begin{pmatrix} e^{i\varphi_{1,2}} & 0 \\ 0 & 1 \end{pmatrix}. \quad (\text{S8})$$

To study the symmetry properties of the unitary evolution operator we symmetrize the matrices $B_{1,2}(k)$ and $D_{1,2}$:

$$B(k) \equiv \begin{pmatrix} e^{-ik/2} & 0 \\ 0 & e^{ik/2} \end{pmatrix}, D(\varphi) \equiv \begin{pmatrix} e^{i\varphi/2} & 0 \\ 0 & e^{-i\varphi/2} \end{pmatrix} \quad (\text{S9})$$

and write

$$\begin{aligned} U_F(k, \varphi) &= e^{i(\varphi_1 + \varphi_2)/2} D(\varphi_2) B(k) S_2 D(\varphi_1) B(k) S_1 \\ &= e^{i(\varphi_1 + \varphi_2)/2} T_2 S_2 T_1 S_1, \end{aligned} \quad (\text{S10})$$

where $T_{1,2} = D(\varphi_{1,2})B(k)$. We notice that both $B(k)$ and $D(\varphi)$ possess inversion symmetry: $\sigma_x B(k) \sigma_x = B(-k)$, $\sigma_x D(\varphi) \sigma_x = D(-\varphi)$, where σ_x is the Pauli matrix. Consequently, for $\varphi_1 + \varphi_2 = 0$ the Floquet evolution operator also has the inversion symmetry $\sigma_x U_F(k, \varphi) \sigma_x = U_F(-k, -\varphi)$. However, introducing a net phase $\varphi_1 + \varphi_2 \neq 0$ over one Floquet period breaks this symmetry and leads to winding of the bands.

III. CALCULATION OF THE TOPOLOGICAL INVARIANT

Given the factorized version of the Floquet evolution operator (S5), we can calculate the topological invariant

$$\begin{aligned} \nu &= \frac{1}{2\pi i} \int_0^{2\pi} d\varphi \text{Tr} \left[U_F^{-1} \frac{\partial U_F}{\partial \varphi} \right] \\ &= \frac{1}{2\pi i} \int_0^{2\pi} d\varphi \text{Tr} \left[S_1^\dagger B_1^\dagger D_1^\dagger S_2^\dagger B_2^\dagger D_2^\dagger \frac{\partial}{\partial \varphi} [D_2 B_2 S_2 D_1 B_1 S_1] \right] \\ &= \frac{1}{2\pi i} \int_0^{2\pi} d\varphi \text{Tr} \left[D_1^\dagger \frac{\partial D_1}{\partial \varphi} + D_2^\dagger \frac{\partial D_2}{\partial \varphi} \right]. \end{aligned} \quad (\text{S11})$$

By substituting (S8) we get

$$\nu = \frac{1}{2\pi i} \int_0^{2\pi} d\varphi [ic_1 + ic_2] = 2K. \quad (\text{S12})$$

IV. HAMILTONIAN FORMALISM

The coherent split step model discussed above in terms of evolution operators can also be described using a time dependent Hamiltonian, as originally discussed in Ref. [S1]. To describe the two step process, we divide each period of the Hamiltonian evolution into four steps:

$$H(t, k_x) = \begin{cases} H_1(k_x) = \begin{pmatrix} 0 & 0 \\ 0 & -V_1 \end{pmatrix}, & 0 < t \leq t_1 \\ H_2(k_x) = \begin{pmatrix} 0 & -J_1 e^{-ik_x/2} \\ -J_1 e^{ik_x/2} & 0 \end{pmatrix} & t_1 < t \leq t_2 \\ H_3(k_x) = \begin{pmatrix} 0 & 0 \\ 0 & -V_2 \end{pmatrix} & t_2 < t \leq t_3 \\ H_4(k_x) = \begin{pmatrix} 0 & -J_2 e^{ik_x/2} \\ -J_2 e^{-ik_x/2} & 0 \end{pmatrix} & t_3 < t \leq T \end{cases} \quad (\text{S13})$$

The parameters V_1, V_2, J_1 and J_2 are related to the phases gained in the left ring and the coupler strengths via:

$$\phi_1 \equiv V_1 \tau_1 / \hbar \quad \theta_1 \equiv J_1 \tau_2 / \hbar \quad \phi_2 \equiv V_2 \tau_3 / \hbar \quad \theta_2 \equiv J_2 \tau_4 / \hbar. \quad (\text{S14})$$

The action of the phase modulator in the first and third steps directly maps into a modification of the onsite energy, while the couplers act as hopping amplitudes. In this way it can be readily seen that the presence of the phase modulation breaks inversion symmetry.

Note that the each time step can be associated to an evolution operator U_j during the duration $\tau_j = t_j - t_{j-1}$:

$$U_j(k_x) \equiv e^{-iH_j(k_x)\tau_j/\hbar}, \quad (\text{S15})$$

so that the evolution (Floquet) operator after one full period is defined as $U_F(k_x) = U_4 U_3 U_2 U_1$, with stepwise evolution operators:

$$U_1 = \begin{pmatrix} 1 & 0 \\ 0 & e^{i\phi_1} \end{pmatrix} \quad U_2 = \begin{pmatrix} \cos \theta_1 & ie^{-ik_x/2} \sin \theta_1 \\ ie^{ik_x/2} \sin \theta_1 & \cos \theta_1 \end{pmatrix} \quad (\text{S16})$$

$$U_3 = \begin{pmatrix} 1 & 0 \\ 0 & e^{i\phi_2} \end{pmatrix} \quad U_4 = \begin{pmatrix} \cos \theta_2 & ie^{-ik_x/2} \sin \theta_2 \\ ie^{ik_x/2} \sin \theta_2 & \cos \theta_2 \end{pmatrix} \quad (\text{S17})$$

leading to the expression of the Floquet operator described in Sec. II.

V. TOPOLOGICALLY PROTECTED BLOCH SUB-OSCILLATIONS

The group velocity in the real space dimension can be found as

$$v_g^\pm(k, \varphi) = \frac{\partial E_\pm(k, \varphi)}{\partial k} = \frac{\pm \cos \theta_1 \cos \theta_2 \sin(k + K\varphi)}{\sqrt{1 - [\cos \theta_1 \cos \theta_2 \cos(k + K\varphi) - \sin \theta_1 \sin \theta_2 \cos(\Delta\varphi)]^2}}$$

Due to the term $\sin(k + K\varphi)$ in the numerator, the sign of v_g changes $2K$ times when φ is changed by 2π , forcing a wavepacket to experience K sub-oscillations during one driving period. Since $\sin(k + K\varphi)$ becomes zero with periodicity of π/K in φ , we can claim that the winding number topologically protects the frequency of Bloch sub-oscillations. At the same time if $K \neq \Delta$, then the term $\cos(k + K\varphi)$ in the denominator precesses at a different rate than $\cos(\Delta\varphi)$. Consequently, the translational symmetry $v_g(k, \varphi) = v_g(k, \varphi + 2\pi/K)$ gets broken, leading to sub-oscillations of different amplitudes.

Finally, the center-of-mass motion of the wavepacket can be found by integrating the group velocity:

$$X(k, t) = \int_0^t v_g(k, \varphi(\tau)) d\tau \quad (\text{S18})$$

VI. EXPERIMENTAL PLATFORM

The photonic network is made of two fiber rings coupled by an electronically-controlled high-bandwidth variable beamsplitter (EOSpace AX-2x2-0MSS-20). Each of the rings contains an erbium-doped fiber amplifier (Keopsys CEFA-C-HG) followed by a narrow-band optical filter (EXFO XTM-50), an isolator, a polarizer, a variable attenuator, and an optical switch (Photonwares NSSW). One of the rings contains a phase electro-optic modulator (EOM, iXblue MPZ-LN-10), which imposes the phases $\varphi_{1,2}$. All the fiber components use polarization-maintaining fibers. Each ring has a length of 40 m, and the length difference between the rings is 0.55 m. The mean length of the two rings sets the round trip period, of 205 ns, between the different time steps m . The length difference sets the temporal size of the lattice sites n in the synthetic spatial dimension, of 2.7 ns.

For the injection of light, emission of a narrow single-frequency laser (IPG Photonics ELR-5-LP) at a wavelength of 1550 nm is chopped into 1.4 ns-long pulses by an amplitude EOM (iXblue MXER-LN-10). Before entering the fiber rings the light passes through an optical switch, which is closed after the injection. This ensures that no spurious signal from the laser enters the fibers during the experiment. The prepared injection signal is coupled into one of the rings through a 70/30 beamsplitter.

VII. MEASUREMENT PROCEDURE

The light field in the system is probed via an 80/20 beamsplitter in each of the rings. To get access to both the amplitude and the phase of each light pulse we use optical heterodyning. For this, a fraction of the laser light is modulated by a phase EOM at a frequency of $\Omega = 3$ GHz, thus creating sidebands shifted by $\pm\Omega$ from the laser frequency. Next, the $+\Omega$ sideband is filtered out by a home-built fiber ring cavity actively locked to this sideband. The filtered out light field is used as a local oscillator, and its beating with the signal from each ring is measured by a fast photodiode (Thorlabs DET08CFC, 5 GHz). Recording the response of the photodiode with a fast oscilloscope (Tektronix MSO64, bandwidth 4 GHz) allows to see the beating, the amplitude and the phase of which directly correspond to the amplitude and the phase of the light field under study. By reshaping the measured signal in a two-dimensional matrix, we can observe the coherent walk in the real space (Fig. 2(a) of the main text). Performing a two-dimensional Fourier transform of the coherent walk gives access to the band structure centered at the frequency Ω of the local oscillator (Fig. 2(b) of the main text).

VIII. RECONSTRUCTION OF THE BAND STRUCTURE

Due to the periodicity of the system in both synthetic dimension and time, its band structure can be obtained simply by calculating the two-dimensional Fourier transform (2DFT) of a split-step coherent walk. An important prerequisite for this is that each site of the walk (α_n^m and β_n^m) is a complex number, which accounts for both the amplitude and the phase of the light field. In our experiment the measured quantity is the beating of the signal with the local oscillator at a constant frequency Ω . This allows us to reconstruct the band structure by performing the 2DFT of the measured signal and offsetting it by the frequency Ω .

The length of an optical fiber is sensitive to the environmental temperature and pressure and can fluctuate over time. For our experiment, this can be thought of as an extra optical phase that the light acquires during its propagation in each fiber ring, which results in a shift of the band structure in both horizontal (δk) and vertical (δE) directions. Over a long time, the length of a fiber ring can change by a few wavelengths. This implies that both δk and δE (which are defined modulo 2π) can change in any possible value, and the observed band structure is shifted by an random amount from the expected position.

However, on a short timescale (tens of milliseconds) the length of each ring changes by less than a few percent of a wavelength. This allows us to calibrate the band structure by performing two consecutive experimental shots within a short time (100 μ s), during which δk and δE stay the same. The first shot implements a simple model without extra phase modulation (i.e. $\varphi = 0$), which has a well-known band structure for given θ_1 and θ_2 :

$$E_{\pm}^{\text{ref}}(k) = \pm \arccos(\cos \theta_1 \cos \theta_2 \cos k) \quad (\text{S19})$$

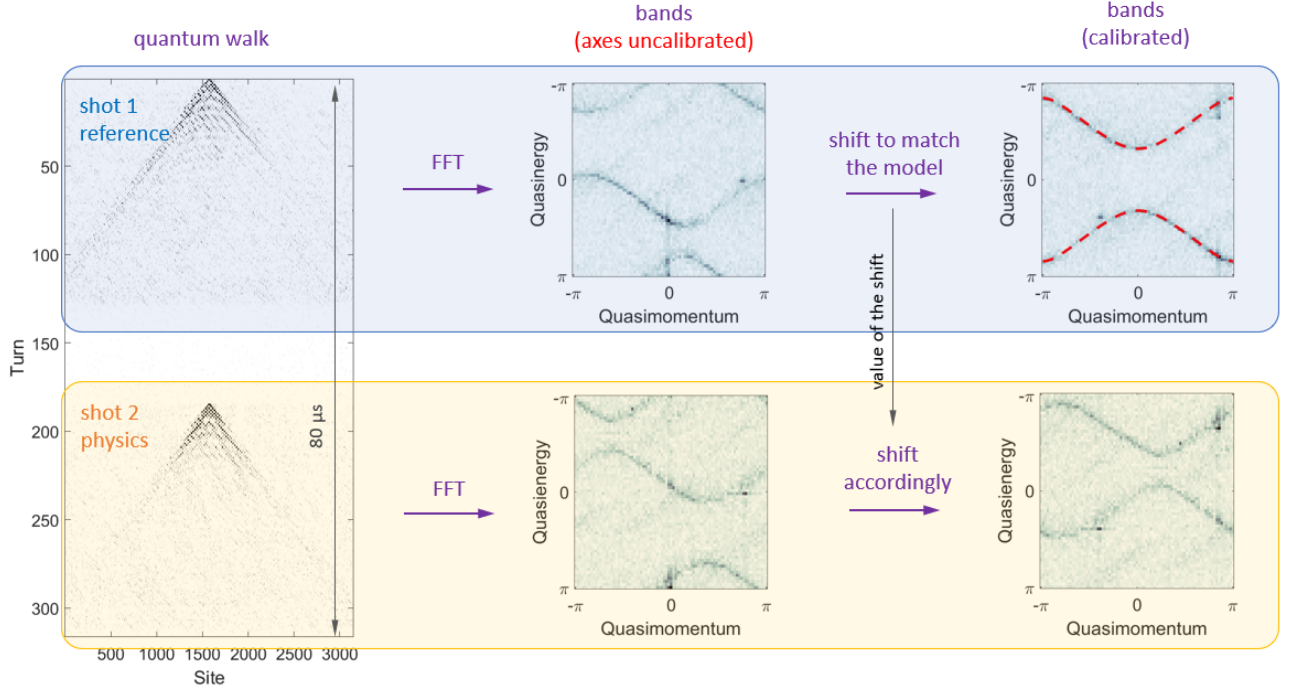


FIG. S1. Calibration of the band structure.

The second shot realizes the experimental system of interest (Fig. S1). By comparing the band structure of the first shot with its theoretical model we can measure the shifts δk and δE and therefore calibrate the axes, which will stay the same during the subsequent shot.

IX. EXCITATION OF A SINGLE BAND

We start with a theoretical description for the case of $\theta_1 = \theta_2 = \pi/4$, which has simple and intuitive analytical expressions for the eigenstates. At time step $m = 0$ we inject a train of pulses with Gaussian envelope into one ring, i.e.

$$\alpha_n^0 = e^{-\frac{n^2}{\sigma^2}}, \quad \beta_n^0 = 0. \quad (\text{S20})$$

Such excitation populates the eigenstates with narrow quasimomentum spread around $k \approx 0$ in both bands. This can be understood knowing that the eigenvectors of the model corresponding to the eigenvalues E_{\pm} are [S2]:

$$\Psi_{\pm} = \begin{pmatrix} A \\ B \end{pmatrix}_{\pm} = \frac{1}{\sqrt{1 + e^{\pm 2 \sin k/2}}} \begin{pmatrix} 1 \\ \mp e^{\pm \sin k/2} e^{-ik/2} \end{pmatrix} \quad (\text{S21})$$

For $k = 0$

$$\Psi_{\pm}(k = 0) = \frac{1}{\sqrt{2}} \begin{pmatrix} 1 \\ \mp 1 \end{pmatrix}, \quad (\text{S22})$$

and for broad Gaussian wavepackets with $\sigma \gg 1$ the excitation (S20) excites equal fraction of both bands at $k = 0$:

$$\begin{pmatrix} \alpha_n^0 \\ \beta_n^0 \end{pmatrix} \approx \begin{pmatrix} 1 \\ 0 \end{pmatrix} = \frac{1}{\sqrt{2}} (\Psi_+ + \Psi_-) \quad (\text{S23})$$

To excite a single band, we program the PM during the turn $m = 1$ to apply a phase $\varphi_1 = \pi/2$. After the first step, the state of the systems becomes

$$\begin{pmatrix} \alpha_{n+1}^1 \\ \beta_{n+1}^1 \end{pmatrix} = \frac{1}{\sqrt{2}} \begin{pmatrix} \alpha_n^0 e^{i\varphi_1} \\ i\alpha_{n+2}^0 \end{pmatrix} \approx \frac{i}{\sqrt{2}} \begin{pmatrix} 1 \\ 1 \end{pmatrix} = i\Psi_-, \quad (\text{S24})$$

and, up to the global phase factor, occupies only one single band Ψ_- . Note that choosing $\varphi_1 = -\pi/2$ would occupy the Ψ_+ band.

For the arbitrary choice of θ_1 and θ_2 one would need to adjust both the phase and the amplitude of signals in two rings in order to excite one single band. However, if chosen values of θ_1 and θ_2 do not alter significantly the shape of the bands (which is the case of our work), one can still transfer the most part of the signal into one band. In our experiment, we can reproducibly inject more than a 80% of the emission into one of the bands (Fig. S2).

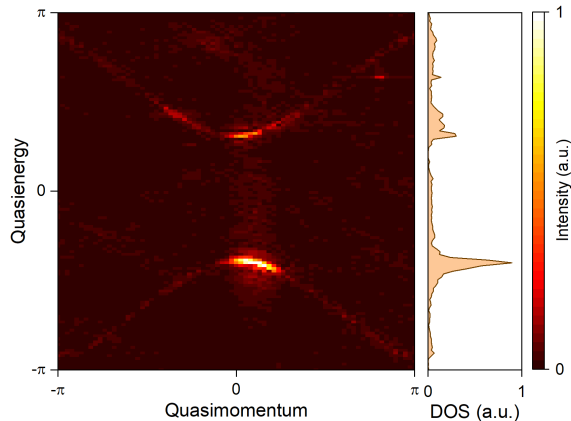


FIG. S2. Excitation of one band

X. IDENTIFICATION OF TRIVIAL AND ANOMALOUS FLOQUET PHASES

To identify the trivial and anomalous Floquet phases we compute the quasienergy spectra $E(k, \varphi)$ for a finite size system containing 50 unit cells along the synthetic dimension with fully reflective boundary conditions. The calculated spectra in the trivial and anomalous case are shown in Fig. S3 A and B respectively. The anomalous phase clearly shows spectral features traversing the gaps, which correspond to the states localized at the edges of the lattice as in Fig. S3C.

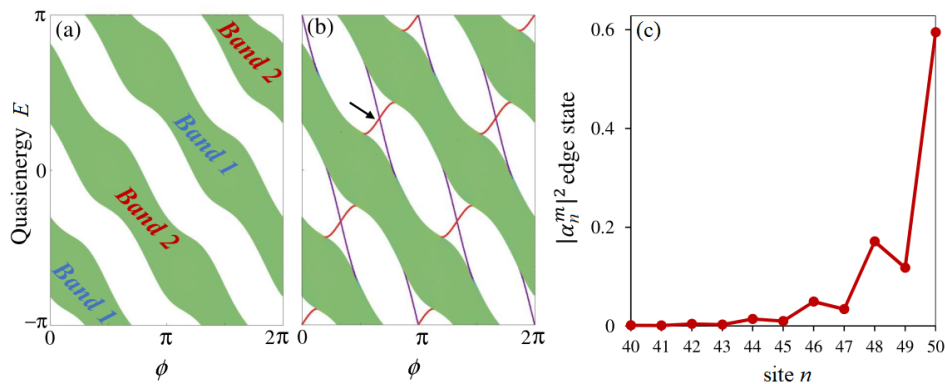


FIG. S3. Calculated bands for the (a) trivial winding metal with $K = -1$, $\theta_1 = \pi/4 - 0.6$, and $\theta_2 = \pi/4$, (b) anomalous winding metal with $K = -1$, $\theta_1 = \pi/4$, and $\theta_2 = \pi/4 - 0.6$. Lines traversing the gap correspond to states localized at the edges. Both models are comprised of 50 sites along the synthetic dimension. (c) Probability amplitude of the red edge state marked by a black arrow in (b) at $\varphi = 1.24\pi$.

-
- [S1] L. K. Upreti, C. Evain, S. Randoux, P. Suret, A. Amo, and P. Delplace, Topological Swing of Bloch Oscillations in Quantum Walks, *Phys. Rev. Lett.* **125**, 186804 (2020).
- [S2] M. Wimmer, A. Regensburger, C. Bersch, M.-A. Miri, S. Batz, G. Onishchukov, D. N. Christodoulides, and U. Peschel, Optical diametric drive acceleration through action–reaction symmetry breaking, *Nat. Phys.* **9**, 780 (2013).